

Supporting Information

Color-tunable tetracoordinated organoboron complexes exhibiting aggregation-induced emission for efficient turn-on detection of fluoride ions

Yanyu Qi,^{a,b} Xiaosong Cao,^a Yang Zou^{*a} and Chuluo Yang^{*a}

^a Shenzhen Key Laboratory of Polymer Science and Technology, College of Materials Science and Engineering, Shenzhen University, Shenzhen 518060, People's Republic of China

^b College of Physics and Optoelectronic Engineering, Shenzhen University, Shenzhen 518060, People's Republic of China

AUTHOR INFORMATION

*Corresponding author. Email: yangzou@szu.edu.cn, clyang@szu.edu.cn

Experimental Section.....	S2
Synthesis.....	S6
Supplementary Figures, Schemes and Tables.....	S8

1. Experimental Section

1.1 Materials. All chemicals and reagents as to be used are of, at least, analytical grade and were purchased from commercial suppliers (Tansoole, Shanghai, China) and used without further purification. Solvents were all dried and degassed using the Grubbs-type solvent purification system, a product of Innovative Technology, Inc. The purified solvents were stored in an argon atmosphere before use. All reactions were monitored by TLC carried out on silica gel plates. Flash column chromatography was performed over silica gel (200-300 mesh). All of the solvents used for fluorescence spectroscopy measurements were freshly distilled before use. 4-(9H-carbazol-9-yl)-phenylboronic acid (Cz-BOH) were obtained from TCI. {4-[9,9-Dimethylacridin-10(9H)-yl]phenyl}-boronic acid (DMAc-BOH) and [4-(10H-Phenoxazin-10-yl)phenyl]boronic acid (PXZ-BOH) were prepared and characterized according to literature procedures.¹ The final products were first purified by column chromatography, then temperature-gradient vacuum sublimation was utilized to further purify target compounds.

1.2 Instrumental Methods. ¹H NMR and ¹³C NMR spectra were acquired on Bruker AV 600 NMR spectrometer at room temperature using CDCl₃ and CD₂Cl₂ as solvent, and referenced externally to SiMe₄. The multiplicities of the signals are indicated as “s”, “d”, “t” or “m”, which stand for singlet, doublet, triplet, and multiplet, respectively. Carbon atoms directly bonded to boron atom are not always observed in the ¹³C NMR spectra due to quadrupolar relaxation leading to considerable signal broadening.² ¹¹B NMR spectra were recorded on Bruker AV 600 NMR spectrometer at room temperature using CDCl₃ as solvent, and chemical shifts (δ) are given in ppm relative to BF₃.OEt₂. ¹⁹F NMR were determined on the same machine using CDCl₃ as solvent to analyze the mechanism. The high-resolution mass spectra (HRMS) were acquired in atmospheric pressure chemical ionization (APCI) sources using a Bruker maXis UHR-TOF mass spectrometer. Single-crystal X-ray Diffraction was obtained using a Bruker D8 Quest Single-crystal X-ray Diffraction spectrometer. UV-Vis spectra were recorded on a UV-3100 spectrophotometer. Steady-state fluorescence excitation and emission spectra were performed at room temperature on a Hitachi F-7000 fluorescence spectrophotometer and a time-correlated single photon counting (TCSPC) Edinburgh FLS 920 fluorescence spectrometer. The absolute fluorescence quantum yields were measured on the time-correlated single photon counting (TCSPC) Edinburgh FLS 920 fluorescence

spectrometer using an integrating sphere. The optical images were recorded using a Canon 70D camera.

1.3 X-ray Crystallography. Crystals of appropriate quality for X-ray diffraction studies were removed and covered with a thin layer of hydrocarbon oil (Paratone-N). A suitable crystal was then selected, attached to a glass fiber. All data were collected using a Bruker APEX II CCD detector/D8 diffractometer using Mo/Cu/Ga $K\alpha$ radiation. The data were corrected for absorption through Gaussian integration from indexing of the crystal faces. Structures were solved using the direct methods programs SHELXS-97, and refinements were completed using the program SHELXL-97.³ The crystallographic information has been deposited with Cambridge Crystallographic Data Centre, and signed to CCDC code 2032300 for **8HQ-Cz**, 2032301 for **8HQ-DMAc**, 2032302 for **8HQ-PXZ** and 2032303 for **8HQ-DMAc-F**.

1.4 Photochemical Stability. The photochemical stability of the representative compounds was tested with a 150W Xenon lamp using a Hitachi F-7000 fluorescence spectrophotometer under the time scan pattern. Typical irradiation times were 2 h.

1.5 Anion sensing studies. Stock solutions (1 mM) of the probes were prepared in THF and the final concentrations were 10 μ M by a 100x dilution of the stock solution. Solutions (0.1 and 1 mM) of the tetrabutylammonium salts of the respective anions were prepared in THF. The concentration of probe compounds was kept constant throughout the titration process, while adding increasing amounts of anion to the probe solution. Then the UV-vis and fluorescence emission spectra were recorded at room temperature. The selectivity properties were explored towards Cl^- , Br^- , I^- , NO_3^- , ClO_4^- , BF_4^- , PF_6^- , AcO^- and H_2PO_4^- (150 μ M) by the sensor concentration in THF in the fluorescence spectra.

1.6 Stoichiometry and Job's plot experiment. Stoichiometry was determined by Job's plot method and monitored by fluorescence spectrometry. Stock solutions of the same concentration (0.2 mM) of the fluorophores and F^- anions were prepared in THF. A series of proportions of F^- varying from 0 to 1.0 was prepared with a constant total concentration (20 μ M). After shaking the vials for a few minutes, the fluorescence emission spectra of the solutions were obtained through fluorescence titration at room temperature. Finally, the intensity changes at relevant maximum emission

wavelength against the concentration ratio of F⁻ to the overall concentration were obtained, namely, the Job's plot.

1.7 Determination of Detection Limit (DL). The detection limit of the sensor has been determined according to the following equations or functions:

$$S_b = \sqrt{\frac{\sum_{i=1}^n (x_i - \bar{x})^2}{n-1}} \quad (1)$$

$$S = \frac{\Delta I}{\Delta c} \quad (2)$$

$$DL = \frac{3S_b}{S} \quad (3)$$

The standard deviation (S_b) regarding present fluorophores and the instrument was determined by measuring the fluorescence intensities (x_i) in THF for more than 100 times, and calculating the corresponding average intensity (\bar{x}) firstly. By fitting the intensity data and the average intensity as obtained into equation (1), the value of the standard deviation (S_b) was obtained.

Then, F⁻ was added into the solution of relevant fluorophores with different concentrations, and then the fluorescence emission intensities were recorded (**Figure 4b, d and f**). Corresponding variations in intensity (ΔI) and the F⁻ concentration (Δc) were calculated. By fitting the data into equation(2), S value for the present system was obtained.

Finally, with the values of S_b and S as determined, the DL for the present system was calculated according to equation (3).

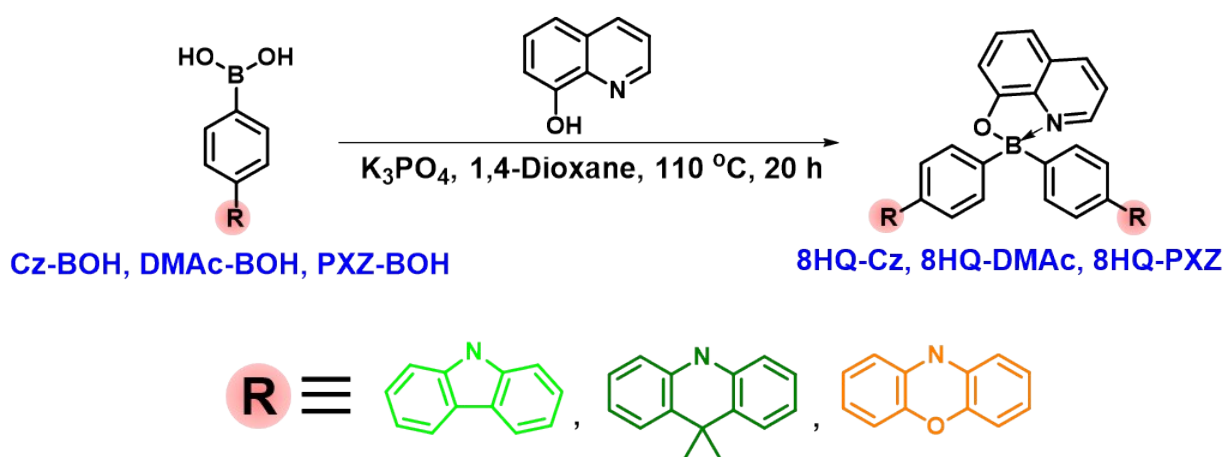
1.8 Preparation of Test Strips. Blank test strips were prepared by cutting ordinary photographic paper (1 cm × 1 cm). The strips as obtained were further treated by immersing them into the THF solution of **8HQ-Cz** (1×10^{-2} mol·L⁻¹), and then dried in air at room temperature.

1.9 Pater Test of F⁻. The aqueous solutions of F⁻ with definite concentrations were prepared by diluting its stock solution (1 mol·L⁻¹) with tap water. Then, the TBAF aqueous solutions as obtained ($1 \times 10^{-6} \sim 1 \times 10^{-1}$ mol·L⁻¹) and tap water were spotted onto the test strips using a micro-syringe. After evaporation of the solvent at room temperature, the test paper was illuminated with handheld UV

light (365 nm). The dark spots were identified by an independent observer, and each set of experiments was repeated three times for consistency.

2. Synthesis

General Procedure for the Synthesis of 8HQ-Cz, 8HQ-DMAc and 8HQ-PXZ: As shown in **Scheme S1**, the fluorophores were synthesized as below: to a 250 mL round bottomed flask equipped with magnetic stirring bar and reflux condenser, 8-hydroxyquinoline (0.29 g, 2.0 mmol), Cz-BOH (5.168 g, 18 mmol), K_3PO_4 (1.28 g, 6.0 mmol) and 1,4-dioxane (100 mL) were added sequentially. The mixture was refluxed for 20 h, and then the solvent was evaporated under reduced pressure. The resulting crude product was taken up in EtOAc (200 mL) and water (20 mL). The separated organic layer was successively washed with 10% aq. K_3PO_4 solution (3×30 mL) and brine (30 mL), dried over anhydrous Na_2SO_4 , and evaporated to dryness under reduced pressure. The residue was purified by column chromatography (Silica, EtOAc/hexanes = 1/9 as eluent) to afford **8HQ-Cz**. **8HQ-DMAc** and **8HQ-PXZ** were synthesized by the same method using DMAc-BOH (5.926 g, 18 mmol) and PXZ-BOH (5.456 g, 18 mmol) to replace Cz-BOH, respectively. Slow evaporation of a solution of the product obtained in hexanes/ $CHCl_3$ at room temperature resulted in crystal of the compound.



Scheme S1. Synthetic route of the fluorophores.

8HQ-Cz. Yellow-green powder (1.1 g, 86%). 1H NMR (600 MHz, CD_2Cl_2 , 25 °C): δ 8.81 (d, 1H), 8.56 (d, 1H), 8.13 (d, 4H), 7.77 (m, 6H), 7.52 (d, 4H), 7.45 (d, 4H), 7.38 (t, 5H), 7.26 (dd, 5H) ppm; ^{13}C NMR (150 MHz, $CDCl_3$, 25 °C): δ 158.6, 146.0, 141.0, 139.5, 139.2, 137.7, 136.6, 133.4, 133.1, 128.6, 126.2, 125.8, 123.3, 123.0, 120.2, 119.7, 112.7, 110.0 ppm; ^{11}B NMR (128.4 MHz, $CDCl_3$, 25 °C): δ 11.14 ppm; HRMS (APCI, m/z, $[M+H]^+$): calcd. for $C_{45}H_{31}BN_3O$: 640.2562, found: 640.2561.

8HQ-DMAc. Yellow powder (0.8 g, 55%). 1H NMR (600 MHz, $CDCl_3$, 25 °C): δ 8.78 (d, 1H), 8.53

(d, 1H), 7.76 (dd, 6H), 7.42 (d, 4H), 7.35 (d, 1H), 7.30 (d, 1H), 7.26 (d, 4H), 6.91 (dt, 8H), 6.32 (d, 4H), 1.67 (s, 12H) ppm; ^{13}C NMR (150 MHz, CDCl_3 , 25 °C): δ 158.6, 141.1, 140.0, 139.5, 139.2, 137.7, 134.4, 133.1, 130.2, 129.8, 128.6, 126.2, 125.0, 123.1, 120.2, 114.2, 112.7, 110.1, 35.9, 31.2 ppm; ^{11}B NMR (128.4 MHz, CDCl_3 , 25 °C): δ 10.77 ppm; HRMS (APCI, m/z, $[\text{M}+\text{H}]^+$): calcd. for $\text{C}_{51}\text{H}_{43}\text{BN}_3\text{O}$: 724.3502, found: 724.3510.

8HQ-PXZ. Orangish red powder (0.55 g, 41%). ^1H NMR (600 MHz, CDCl_3 , 25 °C): δ 8.72 (d, $J = 4.99$ Hz, 1H), 8.53 (d, $J = 8.29$ Hz, 1H), 7.74 (ddd, $J = 6.47, 18.48, 36.74$ Hz, 6H), 7.35 (d, 1H), 7.28 (d, $J = 7.65$ Hz, 1H), 7.24 (s, 2H), 6.59 (m, 14H), 5.94 (d, $J = 6.72$ Hz, 4H) ppm; ^{13}C NMR (150 MHz, CDCl_3 , 25 °C): δ 158.6, 139.4, 139.3, 138.4, 137.7, 136.3, 134.5, 133.2, 131.0, 128.6, 123.0, 113.4, 112.7, 110.1 ppm; ^{11}B NMR (128.4 MHz, CDCl_3 , 25 °C): δ 10.54 ppm; HRMS (APCI, m/z, $[\text{M}+\text{H}]^+$): calcd. for $\text{C}_{45}\text{H}_{31}\text{BN}_3\text{O}_3$: 672.2461, found: 672.2459.

3. Supplementary Figures and Schemes

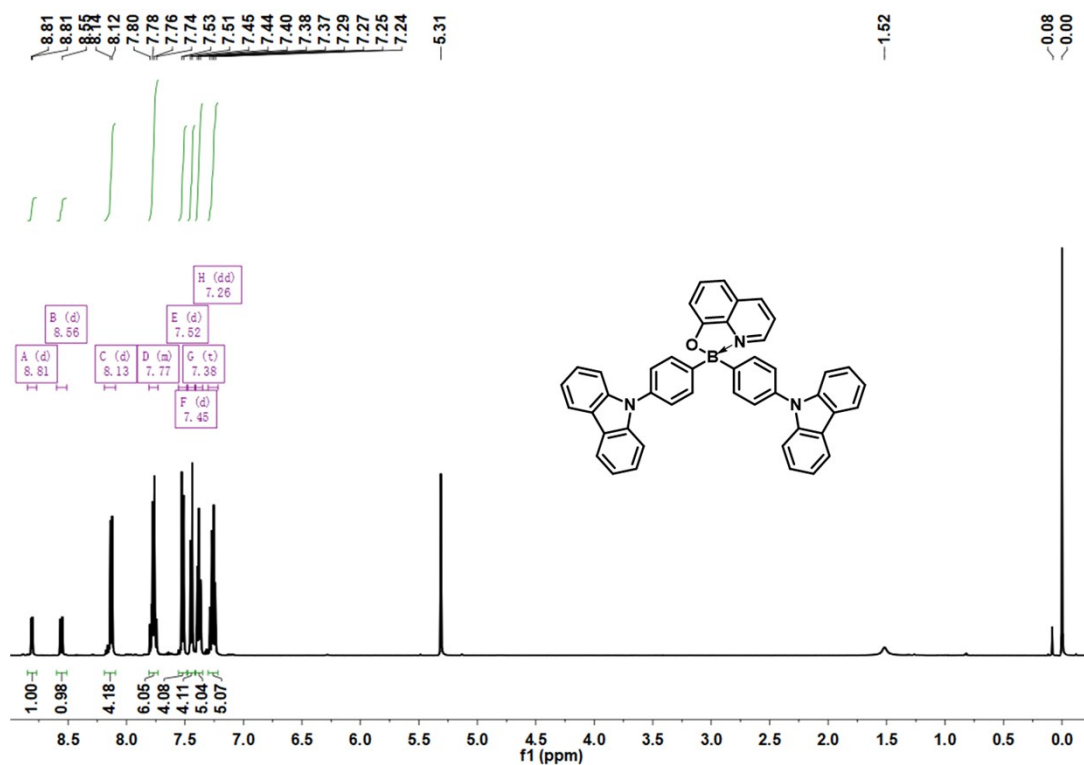


Figure S1. ^1H NMR spectrum of **8HQ-Cz**.

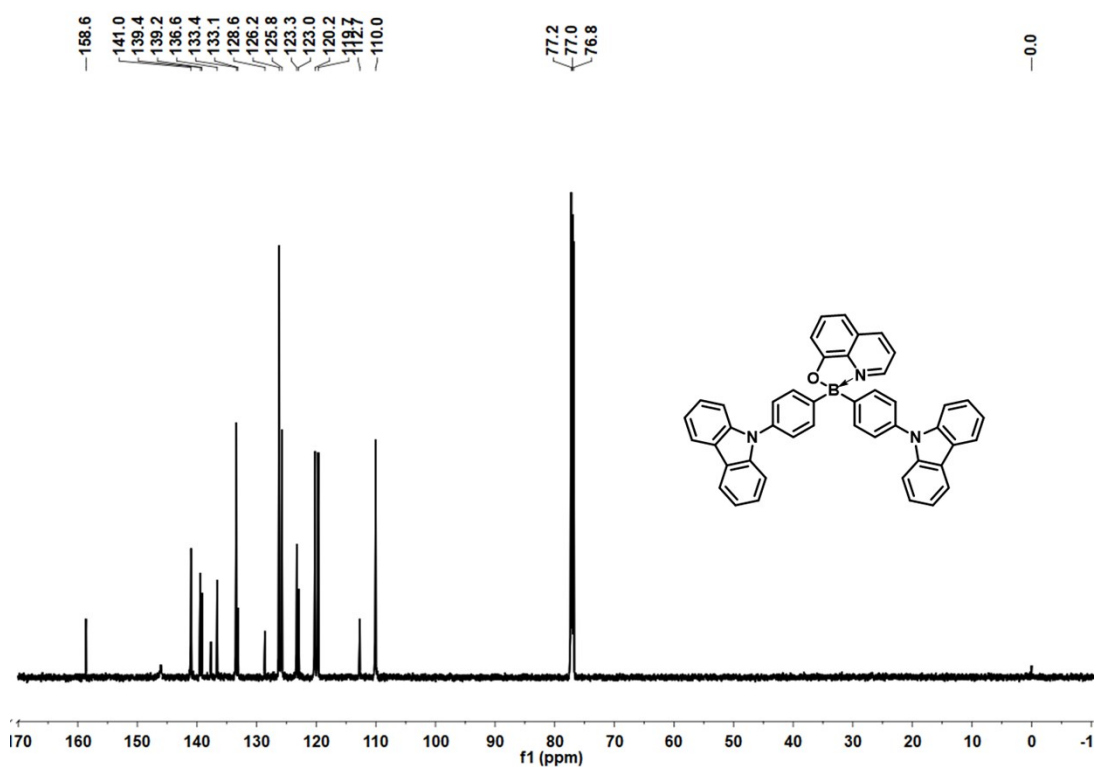


Figure S2. ^{13}C NMR spectrum of **8HQ-Cz**.

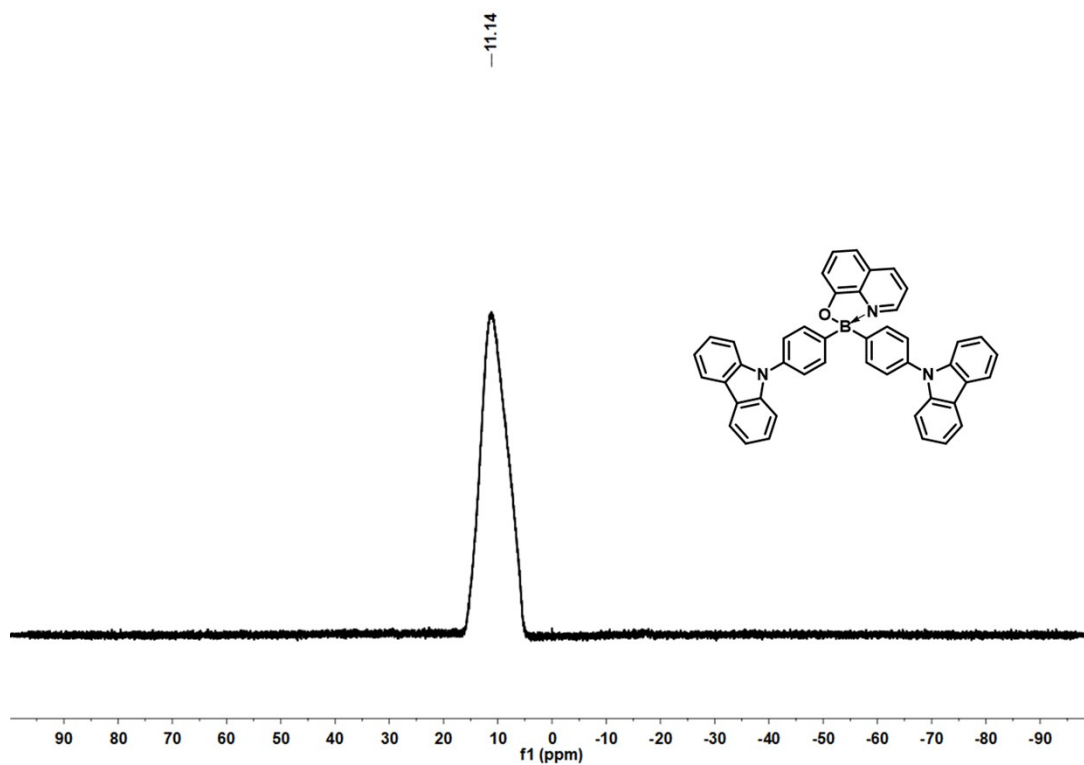


Figure S3. ^{11}B NMR spectrum of 8HQ-Cz.

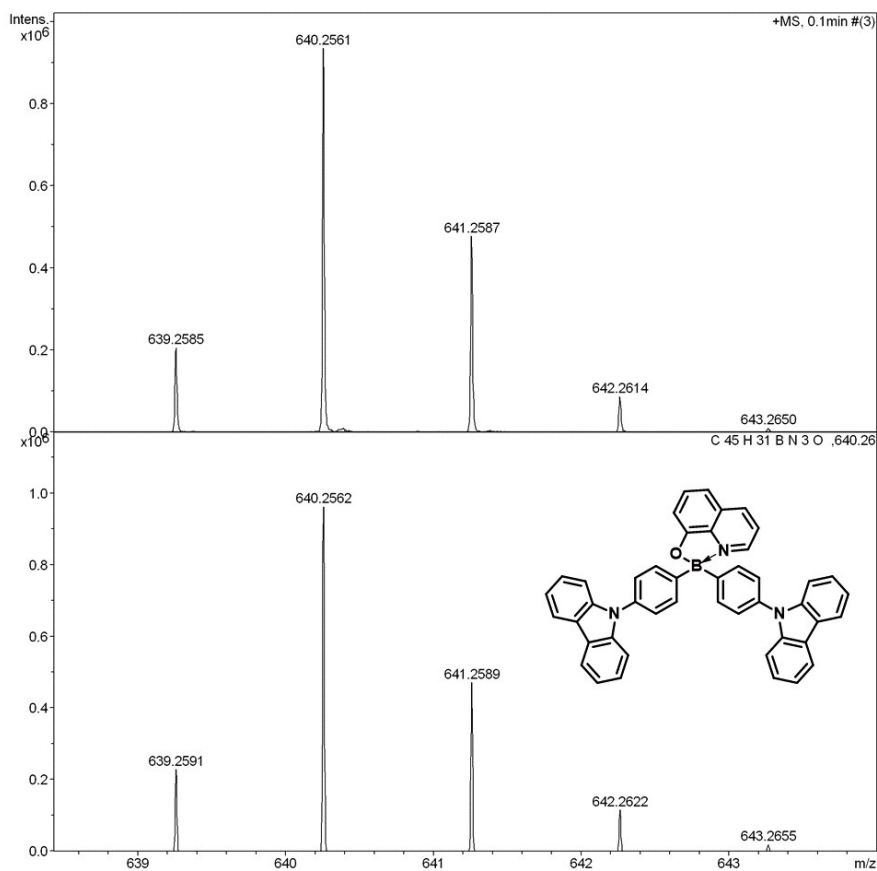


Figure S4. HRMS spectrum of 8HQ-Cz.

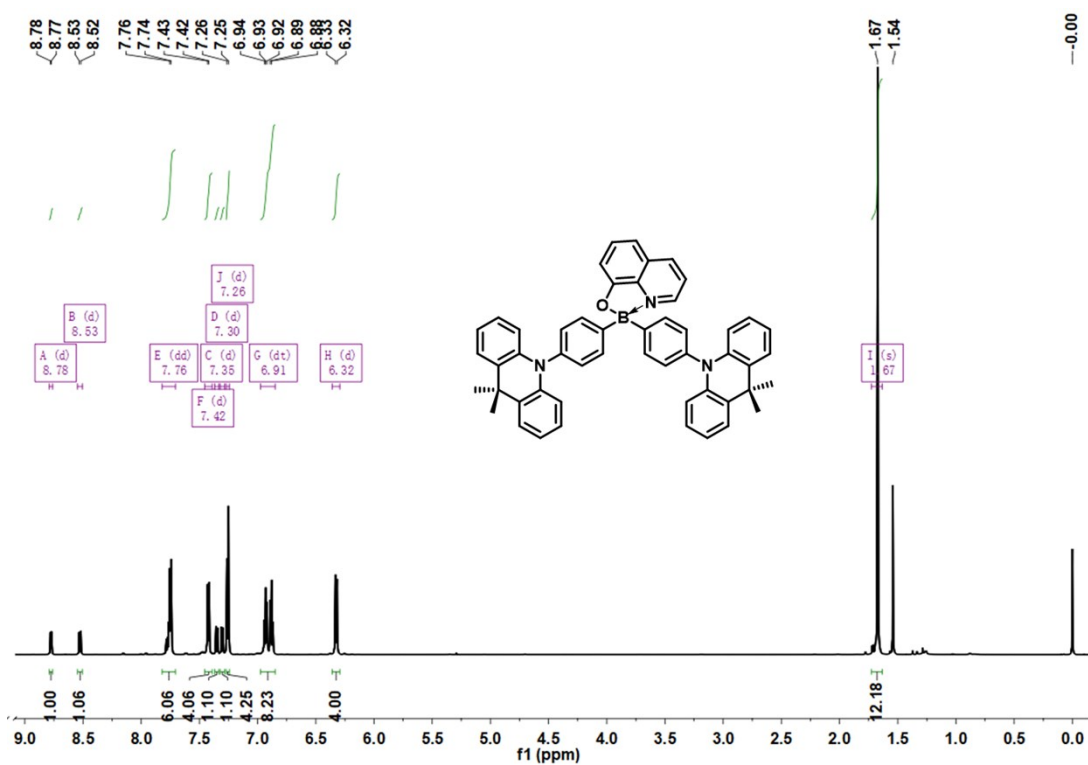


Figure S5. ¹H NMR spectrum of 8HQ-DMAc.

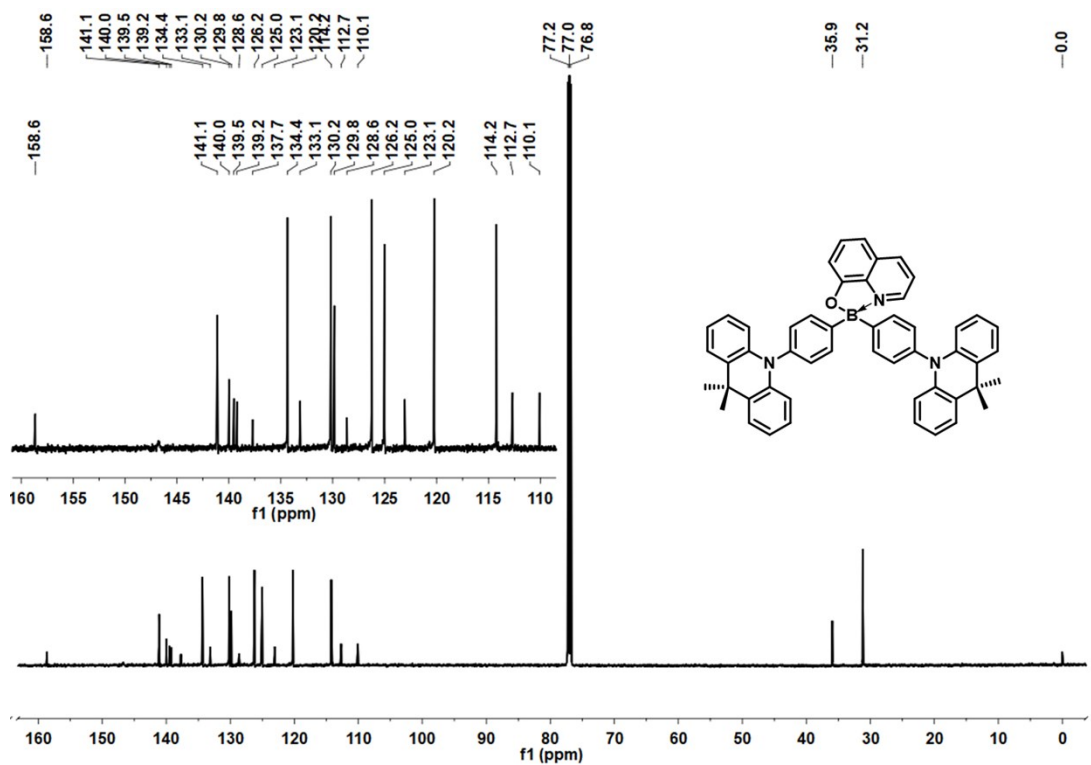


Figure S6. ¹³C NMR spectrum of 8HQ-DMAc.

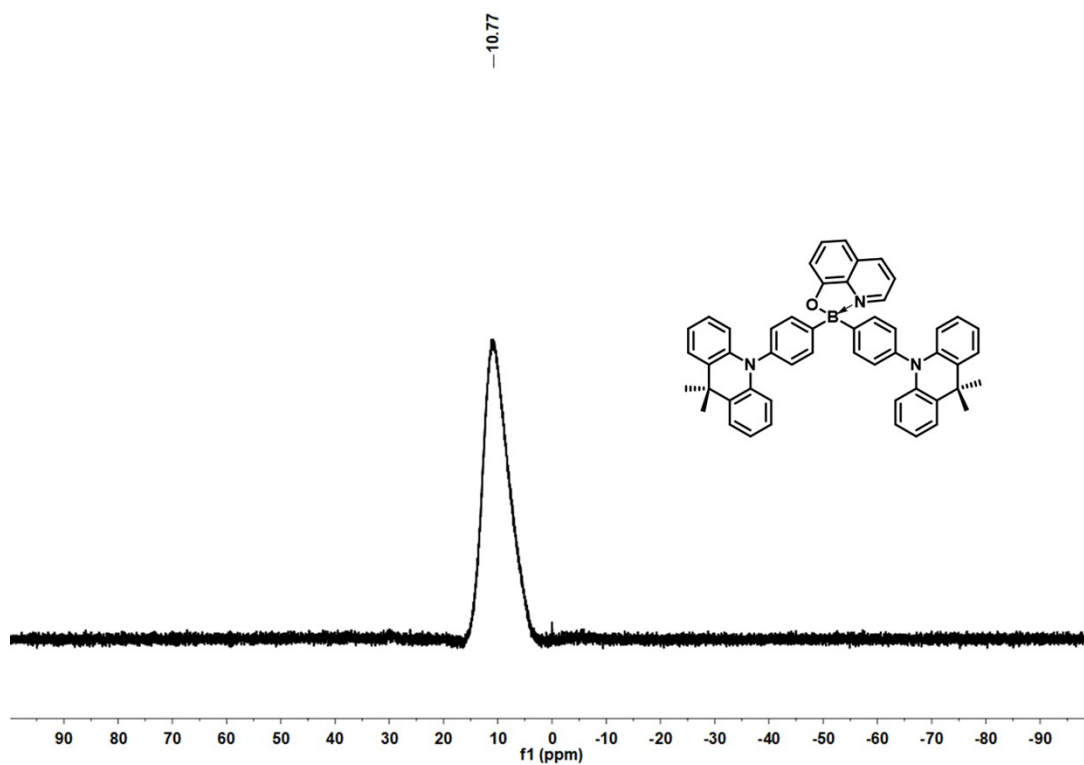


Figure S7. ^{11}B NMR spectrum of **8HQ-DMAc**.

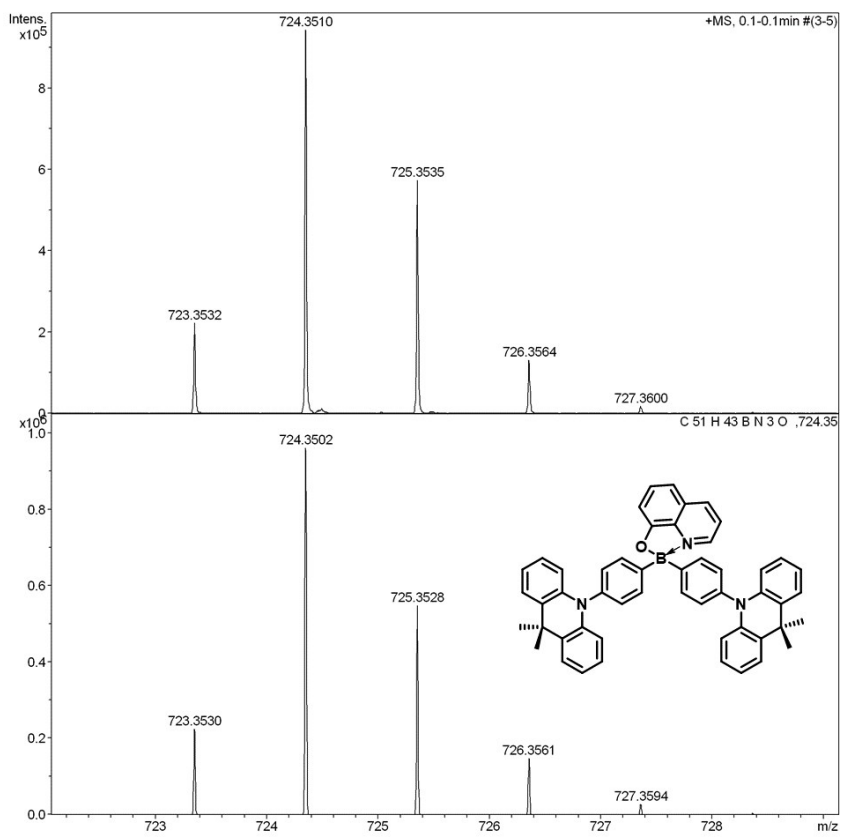


Figure S8. HRMS spectrum of **8HQ-DMAc**.

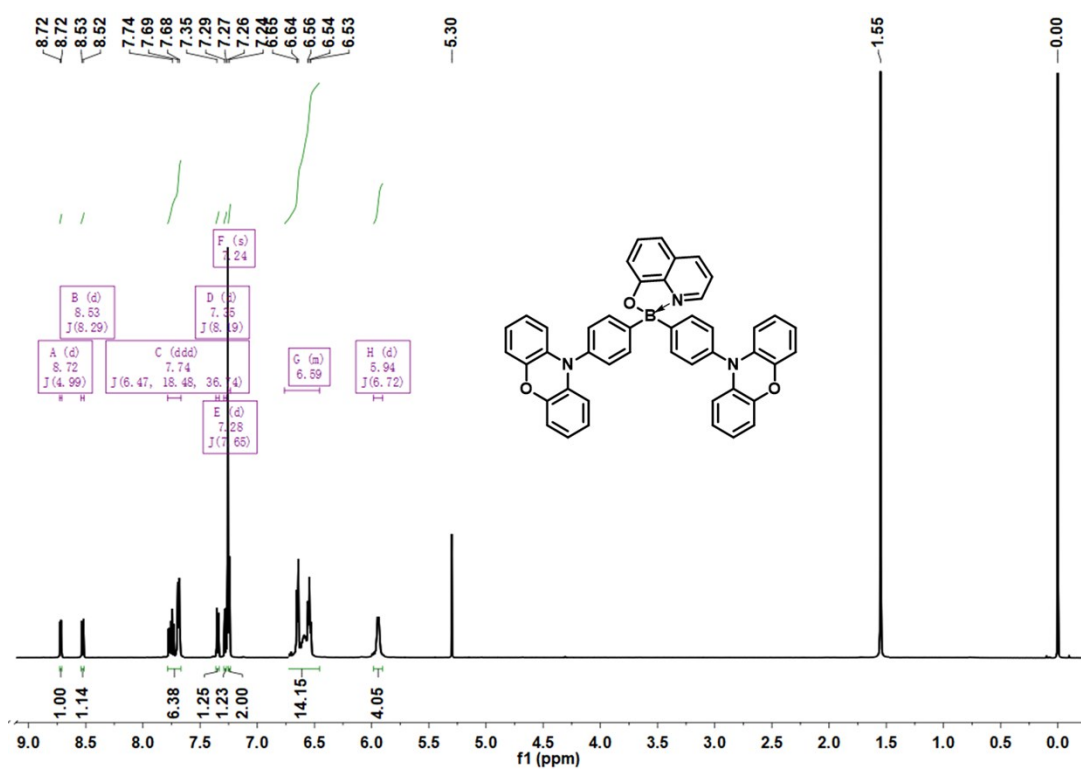


Figure S9. ^1H NMR spectrum of 8HQ-PXZ.

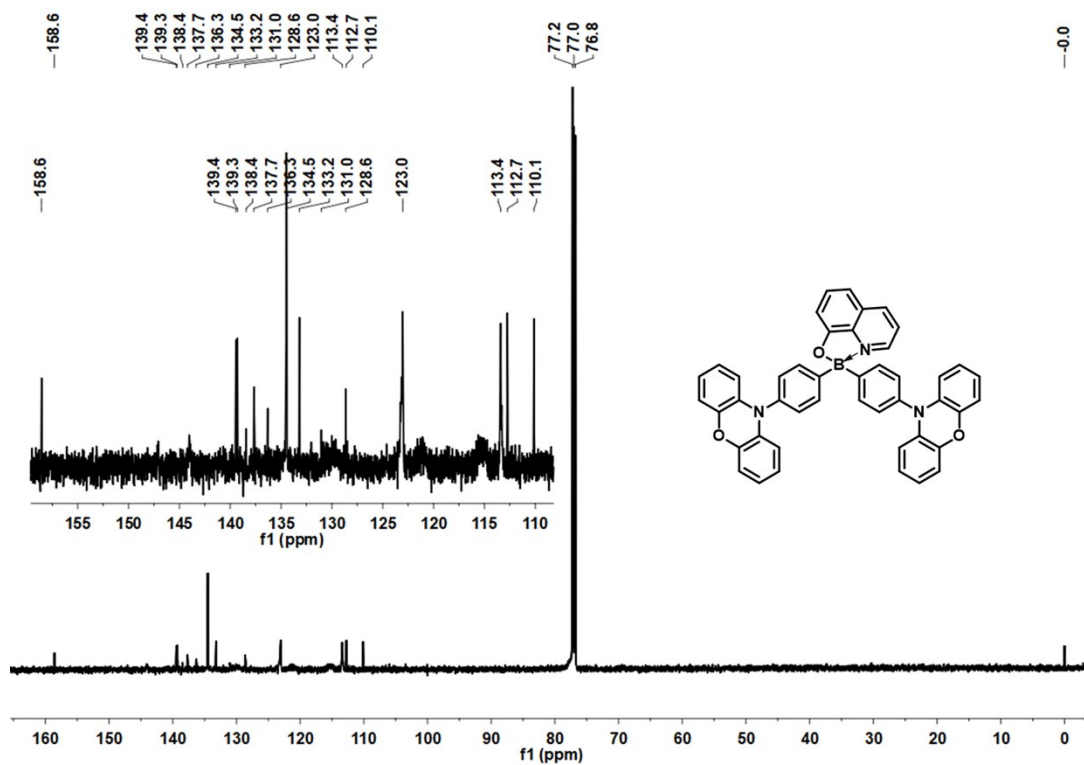


Figure S10. ^{13}C NMR spectrum of 8HQ-PXZ.

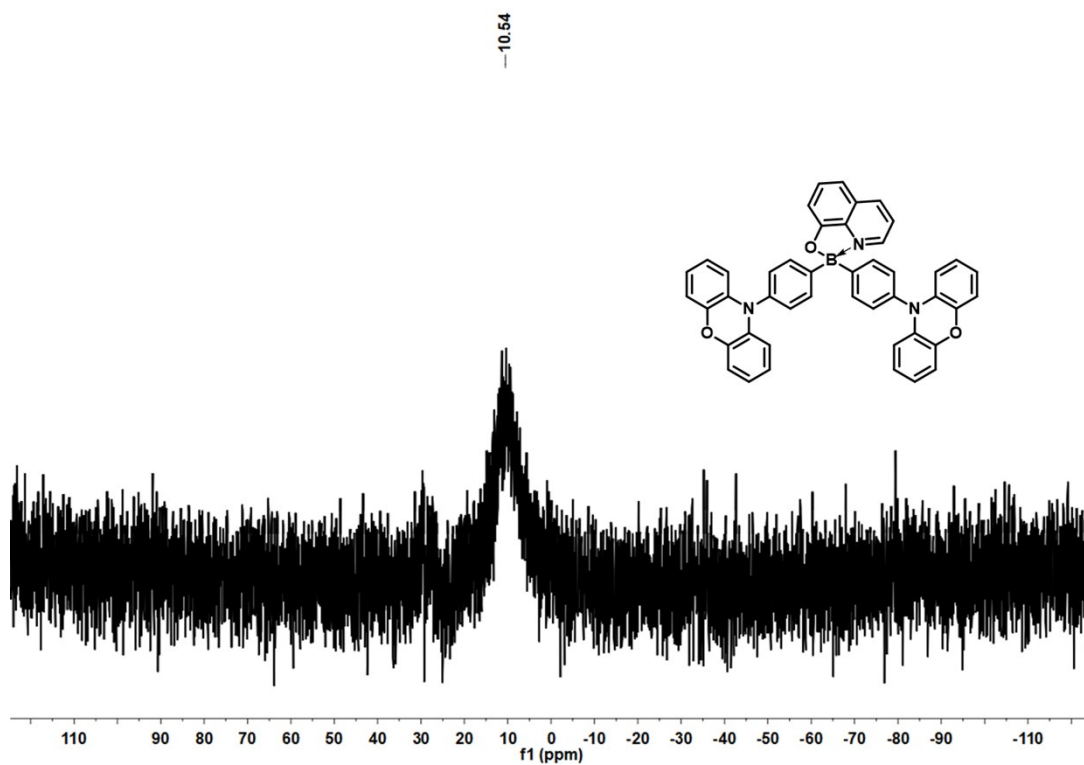


Figure S11. ^{11}B NMR spectrum of **8HQ-PXZ**.

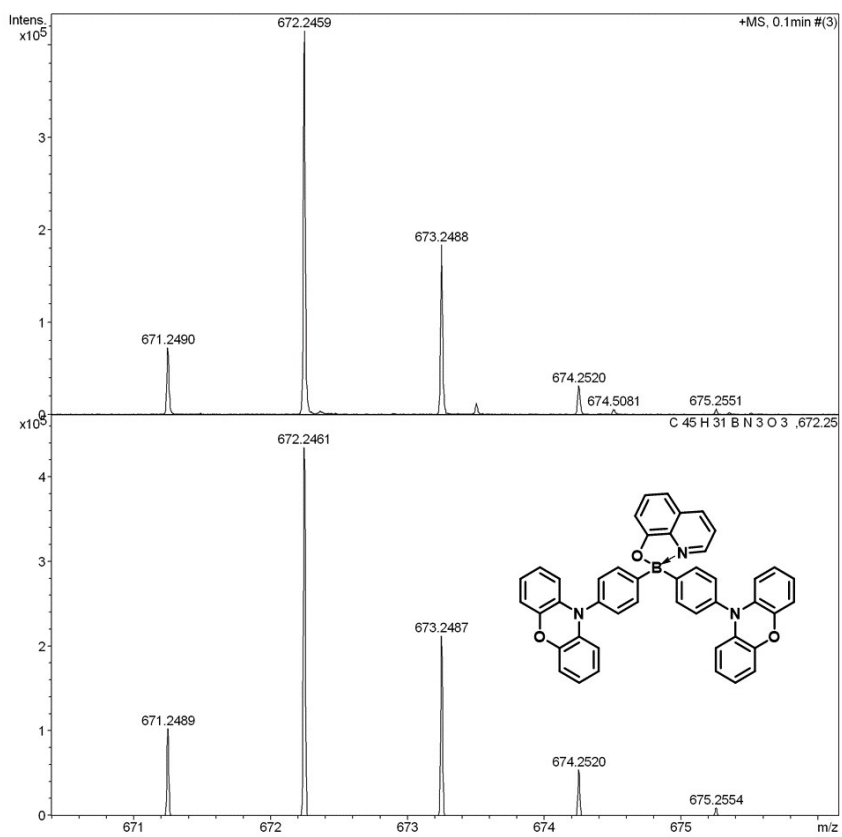


Figure S12. HRMS spectrum of **8HQ-PXZ**.

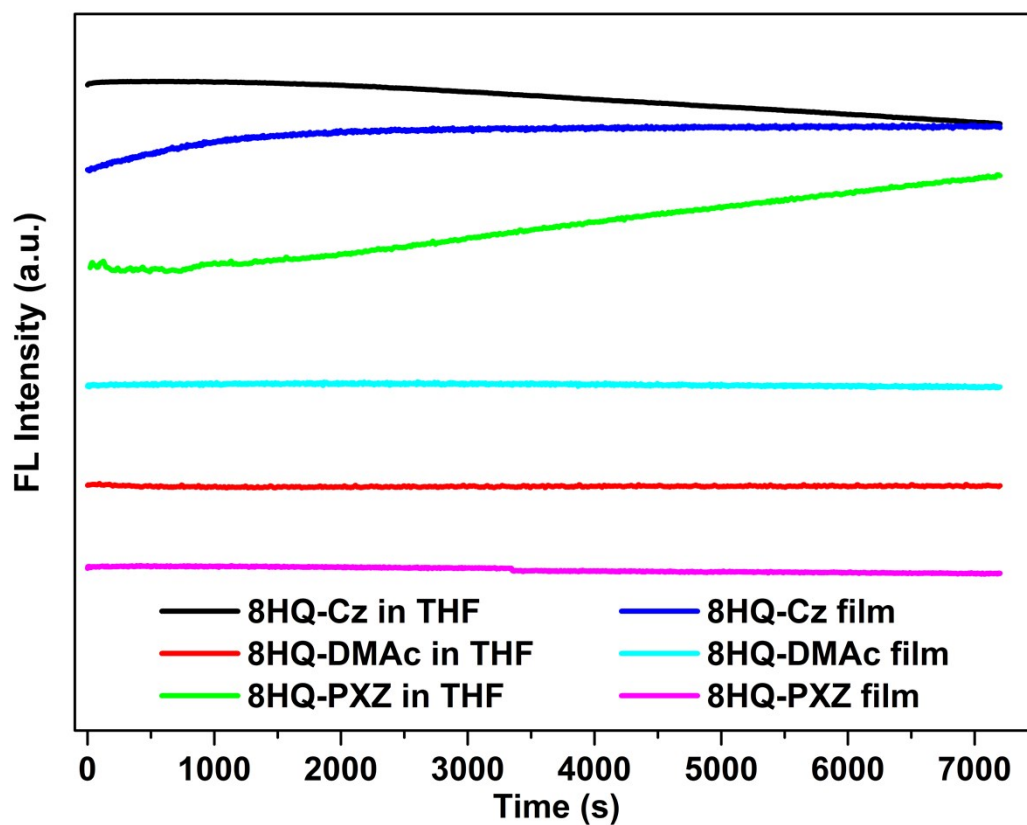


Figure S13. Photochemical stability of **8HQ-Cz**, **8HQ-DMAc**, and **8HQ-PXZ** in THF and thin film states monitored at their maximum emission wavelength with 400 nm as the excitation wavelength.

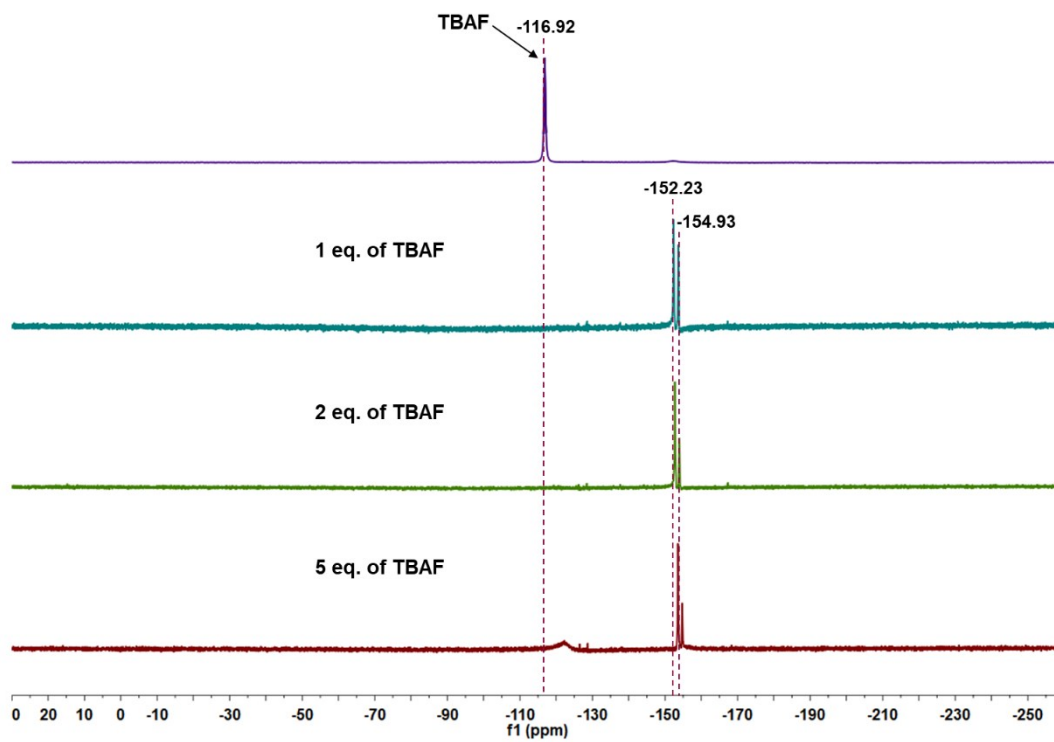


Figure S14. ^{19}F NMR spectra of a mixture of **8HQ-DMAc** after addition of 1, 2 and 5 equiv. of TBAF.

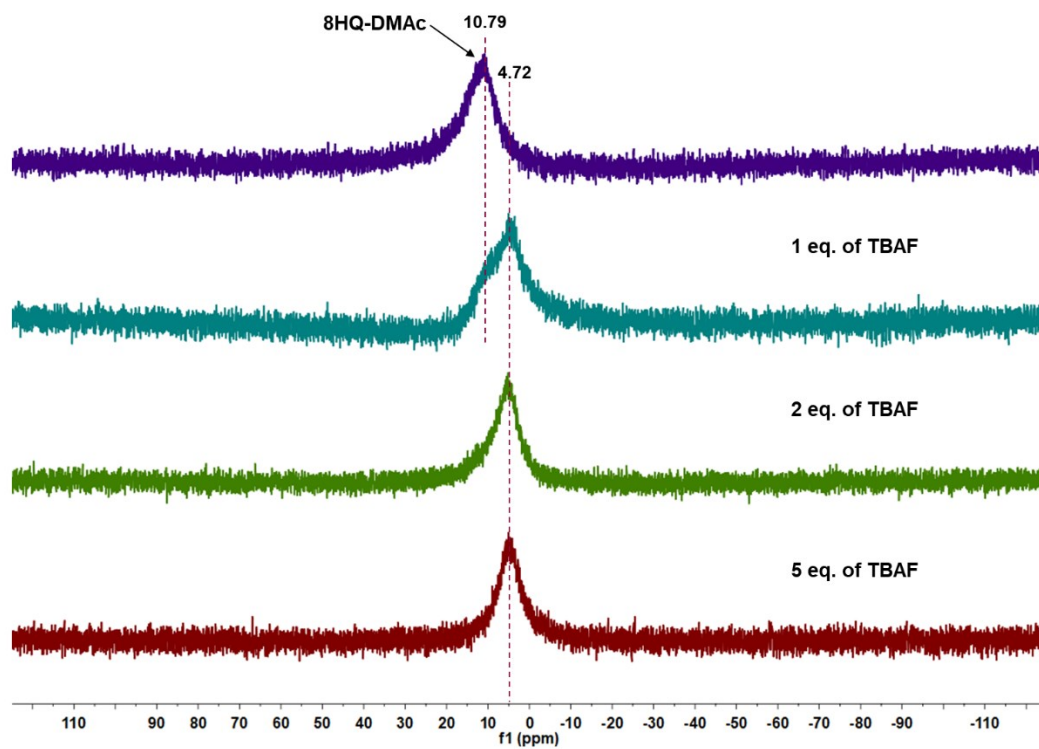
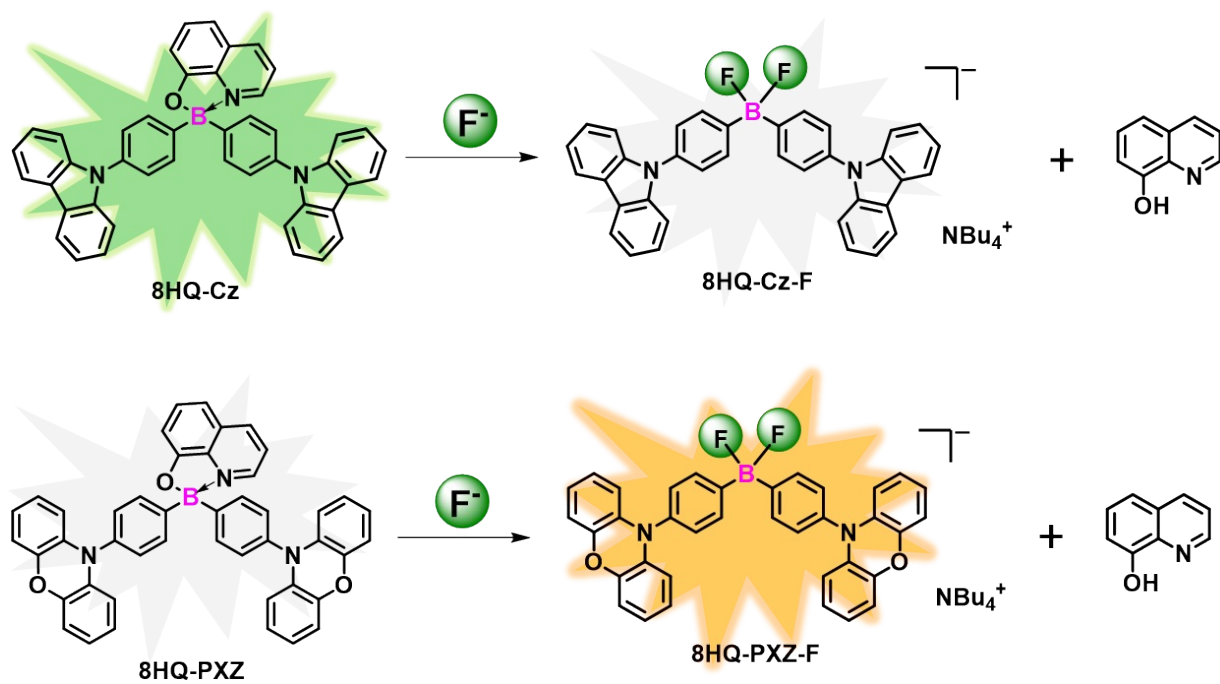


Figure S15. ^{11}B NMR spectra of a mixture of **8HQ-DMAc** after addition of 1, 2 and 5 equiv. of TBAF.



Scheme S2. Schematic illustration of F^- sensing processes using probes **8HQ-Cz** and **8HQ-PXZ**.

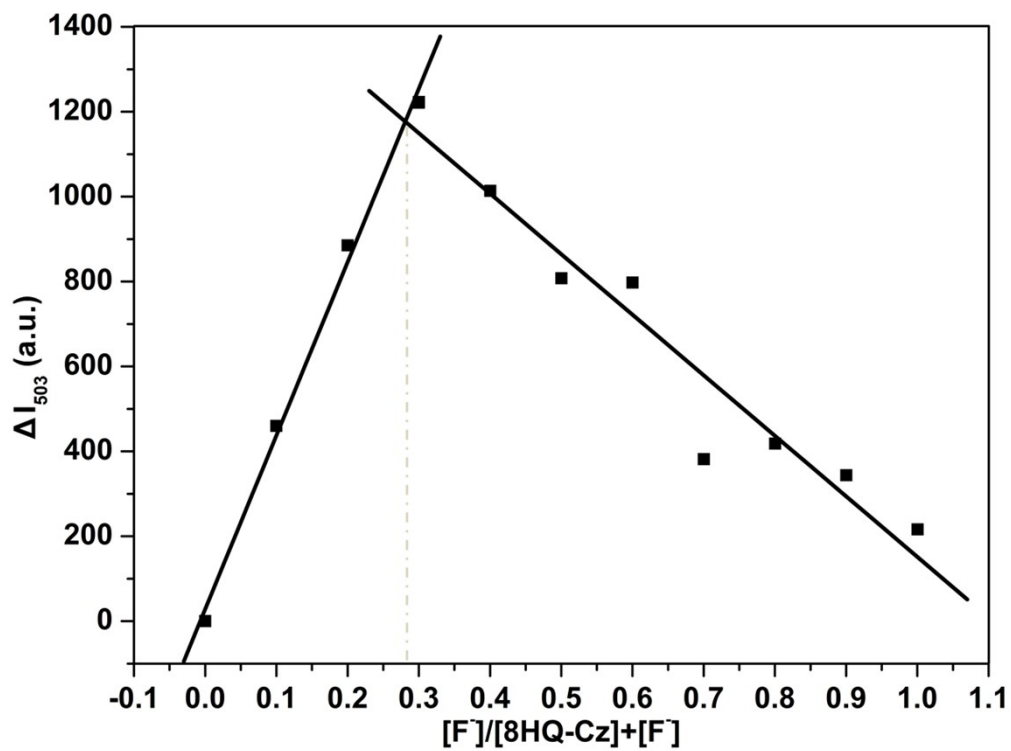


Figure S16. Job's Plot for complexation of **8HQ-Cz** with F^- , the total concentration for the experiments is $20 \mu M$ ($\lambda_{ex} = 400 \text{ nm}$).

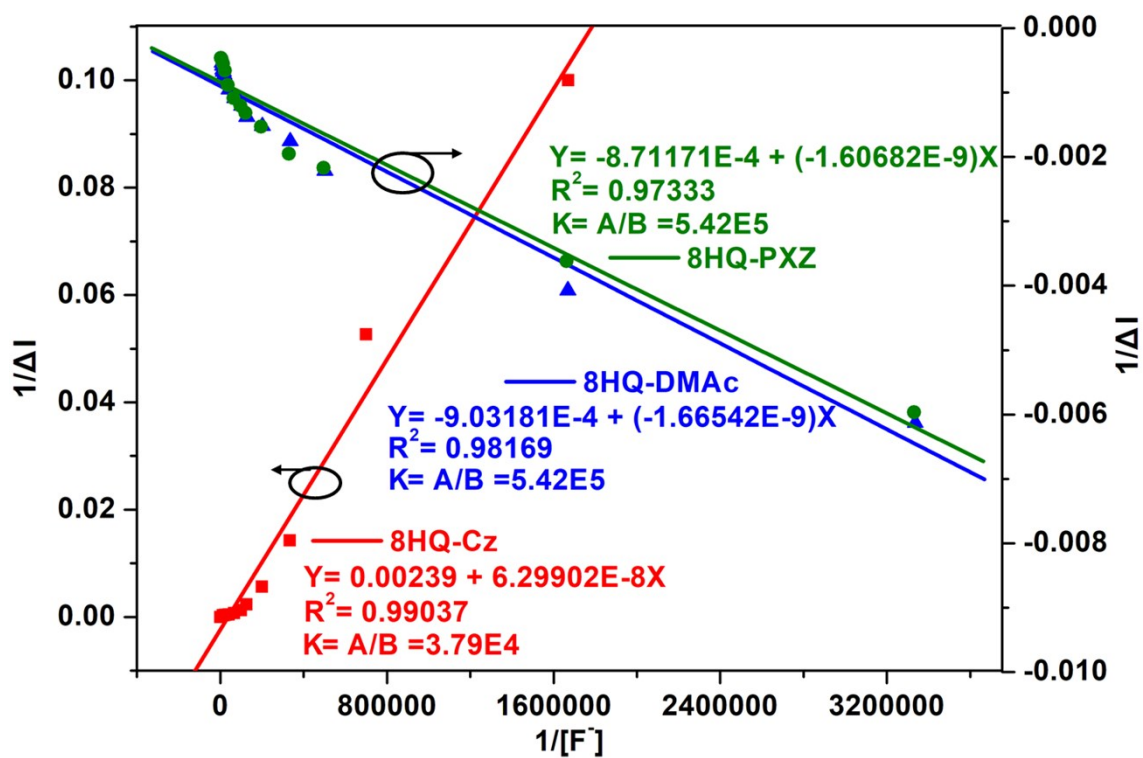


Figure S17. Benesi–Hildebrand plots for complexation of **8HQ-Cz**, **8HQ-DMAc**, and **8HQ-PXZ** with F^- .

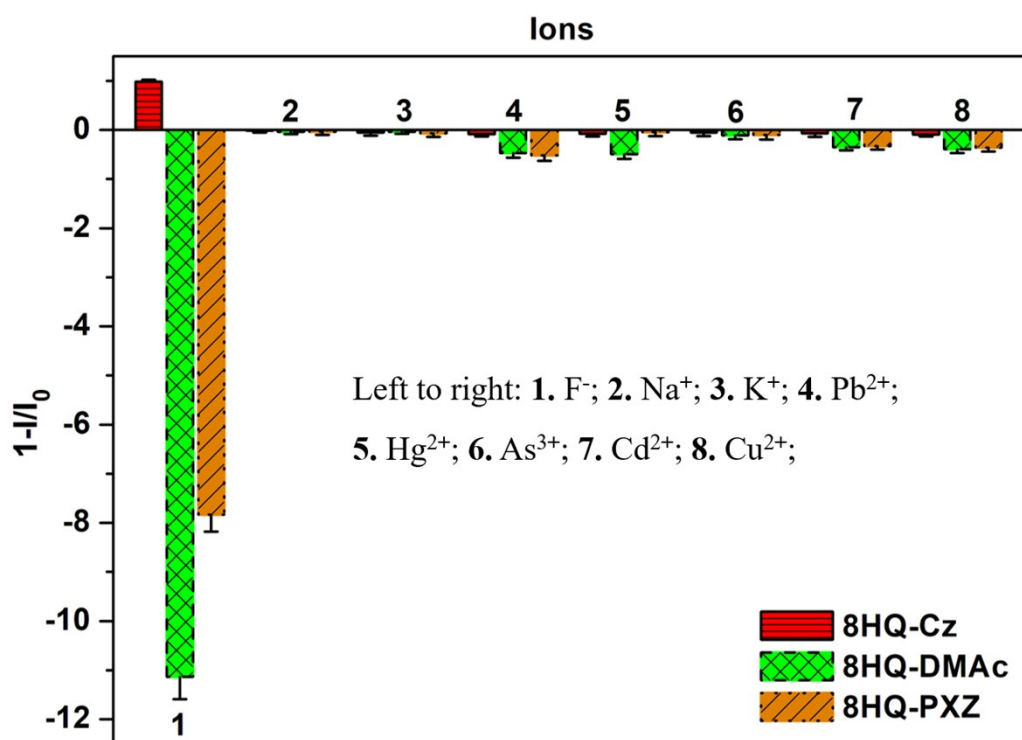


Figure S18. Quantitative histograms of the fluorescence responses of 8HQ-Cz, 8HQ-DMAc, and 8HQ-PXZ, to the presence of F⁻ and different cations (150 μM).

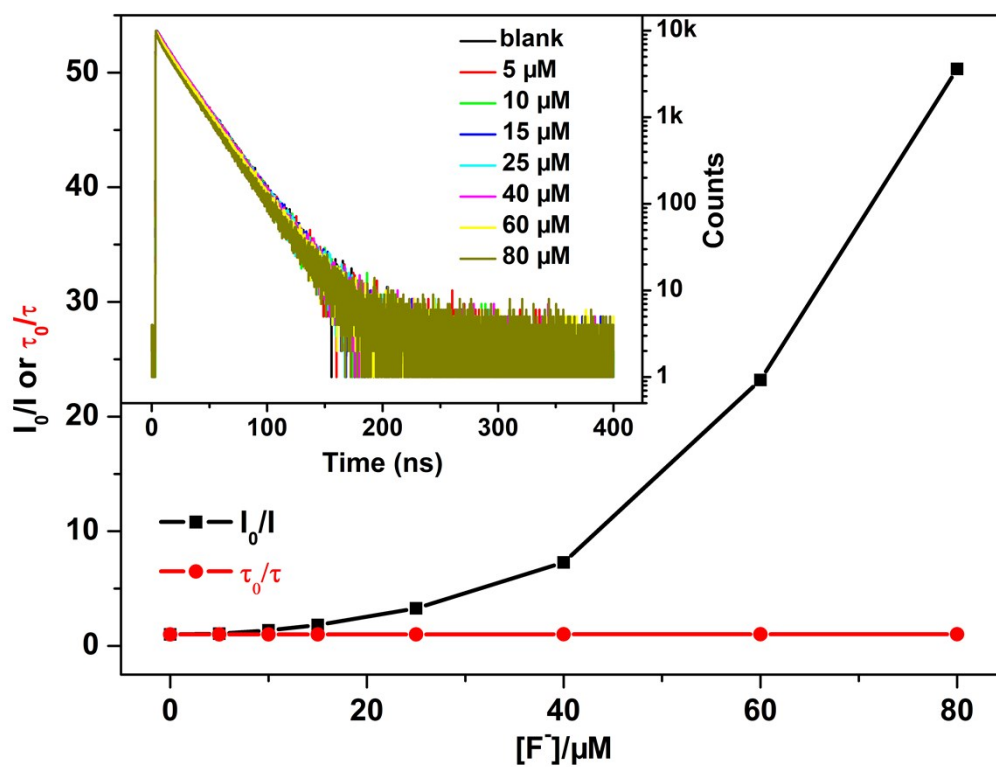


Figure S19. Stern–Volmer plots of fluorescence intensity (I_0/I) and lifetime change (τ_0/τ) as a function of $[F^-]$ of **8HQ-Cz** ($\lambda_{\text{em}} = 503$ nm) in THF upon addition of $n\text{-Bu}_4\text{NF}$.

Table S1. Crystallographic data for **8HQ-Cz**.

Data	8HQ-Cz
CCDC	2032300
formula	C ₄₅ H ₃₀ BN ₃ O
fw	639.53
<i>T</i> /K	293
Wavelength/ Å	1.54184
Crystal system	orthorhombic
Space group	Pna2 ₁
<i>a</i> /Å	15.8969(3)
<i>b</i> /Å	10.4449(2)
<i>c</i> /Å	40.4729(7)
<i>α</i> , deg	90
<i>β</i> , deg	90
<i>γ</i> , deg	90
<i>V</i> /Å ³	6720.2(2)
<i>Z</i> , <i>D_c</i> /(g cm ⁻³)	8, 1.264
<i>μ</i> /mm ⁻¹	0.587
F(000)	2672.0
2θ/deg	8.74 to 151.964
reflns measured	22775
reflns used (<i>R</i> _{int})	10268 (0.0397)
GOF on F ²	1.121
Final <i>R</i> [<i>I</i> > 2σ(<i>I</i>)]	<i>R</i> ₁ = 0.1183 w <i>R</i> ₂ = 0.3364
<i>R</i> (all data)	<i>R</i> ₁ = 0.1351 w <i>R</i> ₂ = 0.3569

Table S2. Crystallographic data for **8HQ-DMAc**.

Data	8HQ-DMAc
CCDC	2032301
formula	C ₅₁ H ₄₂ BN ₃ O
fw	723.68
<i>T</i> /K	293(2)
Wavelength/ Å	1.54178
Crystal system	monoclinic
Space group	C2/c
<i>a</i> /Å	34.5876(5)
<i>b</i> /Å	9.2737(2)
<i>c</i> /Å	13.0117(2)
α , deg	90
β , deg	110.7590(10)
γ , deg	90
<i>V</i> /Å ³	3902.62(12)
<i>Z</i> , <i>D</i> _c /(g cm ⁻³)	4, 1.232
μ /mm ⁻¹	0.561
F(000)	1528.0
2 θ /deg	5.464 to 151.634
reflns measured	12050
reflns used (<i>R</i> _{int})	3861 (0.0201)
GOF on F ²	1.116
Final <i>R</i> [<i>I</i> > 2 σ (<i>I</i>)]	<i>R</i> ₁ = 0.0714 w <i>R</i> ₂ = 0.2051
<i>R</i> (all data)	<i>R</i> ₁ = 0.0758 w <i>R</i> ₂ = 0.2094

Table S3. Crystallographic data for **8HQ-PXZ**.

Data	8HQ-PXZ
CCDC	2032302
formula	C ₄₅ H ₃₀ BN ₃ O ₃
fw	671.53
<i>T</i> /K	170.0
Wavelength/ Å	0.71073
Crystal system	orthorhombic
Space group	Pna2 ₁
<i>a</i> /Å	15.9206(5)
<i>b</i> /Å	10.7686(4)
<i>c</i> /Å	38.8131(12)
α , deg	90
β , deg	90
γ , deg	90
<i>V</i> /Å ³	6654.2(4)
<i>Z</i> , <i>D_c</i> /(g cm ⁻³)	8, 1.341
μ /mm ⁻¹	0.084
F(000)	2800.0
2 θ /deg	3.926 to 52.77
reflns measured	56163
reflns used (<i>R</i> _{int})	13526 (0.1119)
GOF on F ²	1.049
Final <i>R</i> [<i>I</i> > 2 σ (<i>I</i>)]	<i>R</i> ₁ = 0.0616 w <i>R</i> ₂ = 0.1187
<i>R</i> (all data)	<i>R</i> ₁ = 0.1342 w <i>R</i> ₂ = 0.1550

Table S4. Crystallographic data for **8HQ-DMAc-F**.

Data	8HQ-DMAc-F
CCDC	2032303
formula	C ₅₈ H ₇₂ BF ₂ N ₃
fw	859.99
<i>T</i> /K	190(2)
Wavelength/ Å	1.34139
Crystal system	orthorhombic
Space group	P2 ₁ 2 ₁ 2
<i>a</i> /Å	9.8884(14)
<i>b</i> /Å	26.165(4)
<i>c</i> /Å	9.4211(13)
α , deg	90
β , deg	90
γ , deg	90
<i>V</i> /Å ³	2437.5(6)
<i>Z</i> , <i>D_c</i> /(g cm ⁻³)	2, 1.172
μ /mm ⁻¹	0.357
F(000)	928.0
2 θ /deg	5.878 to 113.936
reflns measured	21877
reflns used (<i>R</i> _{int})	4925 (0.0476)
GOF on F ²	1.045
Final <i>R</i> [<i>I</i> > 2 σ (<i>I</i>)]	<i>R</i> ₁ = 0.0448 w <i>R</i> ₂ = 0.1313
<i>R</i> (all data)	<i>R</i> ₁ = 0.0550 w <i>R</i> ₂ = 0.1421

References

- [1] H.-J. Park, S. H. Han, and J. Y. Lee, *Chem. Asian J.*, **2017**, *12*, 2494.
- [2] B. Wrackmeyer, *Prog Nucl Magn Reson Spectrosc.* **1979**, *12*, 227.
- [3] G. Sheldrick, *Acta Crystallogr. A*, **2008**, *64*, 112.